Large-scale shoreline undulations and role of self-organization processes

Xiaojing Zhong[a]*, Ping Dong[b]*, Shenliang Chen[c]**

[a]*School of engineering and Technology, Jimei University, Xiamen 361021, China*

[b]*School of Engineering, University of Liverpool, Liverpool L69 3BX, United Kingdom*

[c]*State Key Laboratory of Estuarine and Coastal Research, East China Normal University, Shanghai 200062, China*

* These authors contributed equally to this work.

**Corresponding author: slchen@sklec.ecnu.edu.cn

ABSTRACT

This study investigates the large scale spatial variation behavior of shoreline changes using the beach profile data along approximately 600 km shoreline around Hainan Island, China. It is found that there exists a power-law relationship between the mean shoreline change variance and the corresponding alongshore scale which holds up to 30 km for the annual shoreline change and reduces to 15 km for seasonal shoreline change. The spatial and seasonal variations of shoreline azimuth, beach sediment size and wave conditions, and their connection with the shoreline change on different scales have been studied. The results suggest that the internal feedback mechanisms between various processes with different spatial scales may be responsible for the observed shoreline change patterns, i.e. the annual shoreline behavior on spatial scale 5-30 km is likely to be the result of self-organization, while the seasonal waves including tropical cyclones and storms exert dominant control of the morphological patterns at spatial scale of 10-25 km.

ADDITIONAL INDEX WORDS: beach; self-affinity; power-law; forcing; seasonal.

Introduction

Coastal evolution involves complicated interactions and often exhibits self-similar (self-affine, fractal) patterns, which can be characterized by power-law scalings. The forms of these patterns are numerous (*e.g.*, beach cusps[1], sand-bars[2, 3], rip-channels[4], and large scale shoreline patterns[5]) and vary in a wide range of spatiotemporal scale. Self-organized processes whose outcomes exhibit power-law scaling, are often observed and applied for modeling[1, 2, 6] and can be easily explained if the spatial scales involved are relatively small. However, the power-law scaling that spans over wide range of scales is much harder to interpret due to the self-organized patterns at different scales may be controlled by different physical processes. This means an unifying explanation for the relationship between variances of coastal morphological changes, such as horizontal movement of shoreline[7] or change of shoreline curvature[8] is presently not available. Therefore, to establish the scale relationships of morphological changes on coasts and underlying mechanisms for these changes, investigations of coastal evolution in a wider range of scales is indispensable. In addition, a better understanding on the connection between power-law scaling and morphological self-organization on coast will be promoted accordingly.

While there exists a comparatively large amount of research on forced coastal forms, the self-organized behavior of coastal morphology in a wide range of scales still needs further exploration and research[9]. Based on analysis of cross-shore profile changes in terms of their self-organizational properties, Southgate and Moller[10] found that when wave conditions were weak or moderate, self-organizational (internal) processes determined the dynamics of the beach profile. The work of Tebbens, Burroughs, and Nelson[7] focused on the shoreline change for tens of kilometers along of the northern North Carolina Outer Banks, United States. The log-log linear relationship between alongshore scale and the variance of horizontal shoreline position change in the cross-shore direction was found to hold for alongshore scales of approximately 100-1,000 m, and a follow-on study by Lazarus *et al.*[8] has extended the scale to up to 8 km. These findings are important as it means that cumulative shoreline evolution process over a period of a year or a few years may exhibit power-law scalings up to a length of 8 km although the underlying processes are unlikely to be scale free.

In this work, the power-law behavior of shoreline changes at large spatial scales is investigated, and possible mechanisms to explain this behavior are explored. The data of horizontal shoreline position change on beach profile used for this study are obtained from three beach profile surveys conducted in a 13-month period along the entire 600 km shoreline around Hainan Island, China. Wavelet analysis are applied to identify the power-law behavior of horizontal shoreline position change and distinguish the shoreline change characteristics at different spatial scale. The standard Empirical Orthogonal Function (EOF) analysis is applied on the elevation data of beach profile to study the variation characteristics of beach morphology in cross-shore direction at various coastal sections, and the analysis results are discussed along with a set of hydrodynamic and geologic conditions in order to shed further light on the underlying mechanisms for the observed shoreline change patterns.

Study area

Hainan Island is located in the South China Sea, separated from Leizhou Peninsula to the north by Qiongzhou Strait (Figure 1). Due to engineering works and urban development at Hainan Island, water and sediment fluxes of rivers on the island decreased slowly in recent 50 years[11]. At present, sediments involved in the coastal evolution around Hainan Island mainly originate from the resuspension of deposited sediment and the erosion of backshore dunes[12]. Sandy coasts are the main shoreline types, and they are separated by bedrock headlands and estuaries (Figure 1 and Table 1). From Hainanjiao to Laoyehai is the east coast with shoreline facing east, and from Laoyehai down to Yinggeju is the south coast.

The climate of Hainan Island and South China Sea is dominated by the East Asian monsoon, with northwest winds during October-March (winter), and south and southeast winds during April-September (summer) [12, 13]. The direction and energy of surface waves around the island are also closely correlated with the seasonal wind direction and forcing strength[12]. Prevailing waves are from northeast in winter and southeast and southwest in summer. In summer season, the Hainan Island is frequently visited by tropical cyclones (about 3 times per year[14]).

Methods

Field survey and data

132 profiles perpendicular to local shoreline around Hainan Island are surveyed, and the distance between every two adjacent profiles is approximately 5 kilometers (Figure 1). Profile elevation measurements were taken with Trimble RTK-GPS 3 times in May 2013 (from 30th April to 14th May, 2013), Dec 2013 (from 6th December to 21st December, 2013) and Jun 2014 (from 6th June to 20th June, 2014). The measuring error is less than 6 cm, which is much smaller than the magnitude of shoreline position variations involved. The latitude and longitude of each profile are recorded in the first survey, and then precisely located in the subsequent surveys. Mean sea level (MSL, 0-m contour) is taken as the representative shoreline position which can be easily and accurately determined by beach survey data[15]. The difference between the distances from the fixed measuring points at the backshore of the profiles to MSL of the two surveys is then taken as the shoreline change. Among the three sets of data for comparison, May2013-Jun2014 (difference of shoreline position between Jun 2014 and May 2013) represents the annual variation of shoreline while May2013-Dec2013 and Dec2013-Jun2014 are the seasonal changes of shoreline.

For each profile measured, five sediment samples were collected along the beach profile starting 2 cm from the top of the profile in the first survey. Sieve analysis is used to obtain particle size distributions of the samples, and the Friedman series formulas[16] are then employed to determine the median grain size (D_{50}) of each sediment sample. D_{50} values from the same profile are averaged to represent the sediment size for the profile.

Shoreline change analysis

The changes in the MSL positions at 132 profiles constitute the shoreline change series around Hainan Island with missing data being filled by linear interpolation. The data is then reconstructed by wavelet transform, which provides information on both the spatial and frequency dependence of a data series. The wavelet analyses are performed using the Wavelet Toolbox in Matlab R2010a. A filter called the Mexican hat wavelet convolves with shoreline change signal, and values for the scale parameter, a, are within the range from 1 to 16. Since the profiles are distributed one after another around the Hainan Island, there is no beginning or ending of the shoreline change signal in the true sense. The profiles are named N001 to N132, and then the term N001 to N132 are repeated three times in sequence to form the signal used for wavelet transform, that is: N001, N002 … N132, N001, N002 … N132, N001, N002 … N132. Only the middle part of coefficient series obtained is used, so that the results are not affected by the edge effect of wavelet transform. The power-spectral exponent, β, is the slope of log-log plot of the variance of wavelet transform coefficients, V, and the wavelet scale, a.

Beach profiles analysis

The EOF analysis is applied to investigate beach profile features of different coastal sections in different time. Each profile is transformed into a set of elevation data with a spatial interval of 1.5 m, starting from MSL. For unifying the length of different profiles, the landward blank elevation data are filled with the elevation of the farthest point measured, which usually is the highest point for those shorter profiles. Hence there are 100 elevation variables on each profile while the unified profile length is 150 meters. The 132 profiles, each with 100 elevation variables, constitute a multivariate matrix fed to the EOF analysis. For unified profile elevation data from the same survey, four beach topography data matrixes used for the EOF analysis are obtained: one matrix contains all the profiles around Hainan Island (N001~N132), and three matrixes for east coast (N010~N049), south coast (N049~N087) and the north & west coast (N088~N009) separately. In total 12 matrixes are generated for three surveys. The calculation procedures followed closely the work of Vincent *et al.*[17].

Hydrodynamic and geological conditions

Routes of tropical cyclones are accessed from Best Track Data by RSMC Tokyo - Typhoon Center (www.jma.go.jp). Significant wave height and wave direction around Hainan during the investigated period are accessed from hourly forecast data of WaveWatch III (WW3) Global Wave Model (oos.soest.hawaii.edu/erddap), which has taken account of the weather conditions including tropical cyclones. While the resolution of WW3 Global wave model is 0.5 degree of longitude/latitude, the modeling points of wave conditions are mostly located in deep water or far away from the shoreline. Therefore, in analyzing the wave effects on the shoreline change patterns, the seasonal significant wave heights along coast of Hainan predicted by Zhou *et al.*[18] is also used.

Since the surveyed beach profiles are perpendicular to local shoreline, the azimuths of these investigated profiles can represent the orientation of the local shoreline around Hainan Island. Azimuths of investigated profiles are calculated from GPS data. To examine the spatial scale of shoreline orientation variation along the coast, wavelet transform is used to analyze the azimuth data series.

Results

Rhythmic shoreline changes at different scales

Shoreline change signals exhibit a rhythmic pattern of alternating seaward and shoreward movements alongshore (Figure 2(a)). At most survey positions, the shoreline moves in opposite directions in the two seasons (May2013-Dec2013 and Dec2013-Jun2014) considered. The contrast between the wavelet transformed results of two seasonal shoreline change signals is also clearly evident (Figure 2(b) and 2(c)): the coast which moved shoreward from summer to winter (May2013-Dec2013) usually changed to moving seaward from the winter to the following summer (Dec2013-Jun2014), and vice versa. The spatial periodic variations in the shoreline change series are clearly strong on different spatial scales.

The variations of shoreline change signals at different sections around Hainan Island are quite different as shown in Figure 2. The shaded parts are the south & east coast, and the cyclic variation there is more pronounced than the rest. In other words, the shoreline at south & east coast is more unstable than north & west coast, except the three abnormal profiles (Figure 2(a)): N104, N118 and N123. Profiles N104 and N123 have underwater shoal and mangrove, which may cause large changes in the local shoreline position. As to profile N118, it is affected by an artificial island located besides it, which was newly built after the first survey. Other profiles at north & west coast did not change much in shoreline position. Subsequent discussion will put particular emphasis on the south & east coast (profiles N010-N087).

Relationships between wavelet coefficient variance and spatial scale of shoreline changes

The relationships between the wavelet transform coefficient variance and the spatial scale of shoreline change series at south & east coast are shown in Figure 3 by log-log plots. In the left graph, the wavelet coefficient variance of annual shoreline change, May2013-Jun2014, rises continually at alongshore scale from 5 km to 30 km, and increases again in the scale range of 60-80 km after dropping at 35-60 km. In contrast the rising trends of seasonal change series, May2013-Dec2013 and Dec2013-Jun2014, break off in the scale range of 10-25 km, and then increase again up to scale around 60 km. The power-spectral exponent, β, of annual shoreline change is steady over the scale range of 5-30 km. The power-law relationships of seasonal shoreline change are also strong with exponent β larger than 1 in the spatial scale up to 15 km.

Cross-shore profile change characteristics

The EOF analysis reveals that first and second eigenvectors can explain over 90% variation of profile elevation (Table 2). The first eigenvectors show the prevailing beach profile forms, and the second eigenvectors reflect the subsequent beach elevation changes along the profiles. In Figure 4(b) and 4(c), it can be clearly seen that the shapes of eigenvectors of winter profiles (Dec2013) are quite different from that of summer profiles (May2013 and Jun2014) for all profiles, which implies seasonal morphological changes on Hainan coasts.

The large variation of eigenvector weighting also indicates significant changes of beach profile, *e.g.* the second eigenvector weightings of profiles from N40 to N70 vary notably between surveys (Figure 4(a)). On the other hand, profiles alongshore with close eigenvector weightings suggest they have similar relationships with eigenvector. Therefore subsections of coast can be recognized by differences in the weightings on alongshore profiles, and the coastal sections divided on this basis corresponds well with the geological conditions (Table 1).

Hydrodynamic conditions

For the south & east coast of Hainan, the direction of incident wave in deep water is almost uniform alongshore with no discernable rhythmic patterns as it can be seen in Figure 1. Furthermore, the annual significant wave height distribution in the coastal area considered is also rather similar, varying within the range of 0.6-1.2 meter (Figure 5 (a)). As shown in Figure 1, along the east and south coast of Hainan, the prevailing wave direction is east-northeast in two seasons, while a proportion of waves coming from south in May2013-Dec2013 changes to east in Dec2013-Jun2014.

During the survey period, there were five tropical cyclones that passed Hainan Island (Figure 1 and Table 3). All these cyclones approached Hainan from the east and south coasts between surveys in May 2013 and Dec 2013, and the last cyclone passed east coast was 4 months before the survey in Dec 2013 while the last cyclone affected south coast only 25 days before 6th Dec 2013. Among the five cyclones, HAIYAN is the strongest and largest one (Table 3), and all of them are strong enough to affect the hydrodynamic conditions at some parts of Hainan coast. The cyclones generated high waves over a wide area, which can be recognized from wave conditions on both southeast coast and west coast (Figure 5(b) and 5(c)). Based on the modelling wave conditions in 18.5°N, 110.5°E (*P1*) and 19°N, 108.5°E (*P2*), it can be concluded that the survey in Dec 2013 was affected by waves with relatively higher significant wave height induced by a series of storms, while the surveys in May 2013 and Jun 2014 were taken after a prolonged period of low waves.

Geological conditions

As shown in Figure 1, most profiles in the survey are on sandy beaches, only a few of them are covered by very fine gravel. It can also be found that the sediments from each single bay are nearly of the same size, but differ significantly from that in the adjacent bays. The bays with alongshore length around 30-40 km are separated by protruding shoreline. As it can be seen in Figure 6, at the spatial scales under 20 km, the variation trends of shoreline change and azimuth are very different from one another (Figure 6(a)), and the Pearson product-moment correlation coefficient between them is only 0.21, which means they are barely correlated. At scale of 40 km alongshore the correlation is more discernible but remains weak (Figure 6(b)) while at scale of 80 km alongshore (Figure 6(c)), the azimuth displays similar trends with shoreline change signal.

Discussion

The phenomena that shoreline changes driven by seemingly different processes can exhibit a consistent trend across a wider range of scales in a power spectrum is indeed both interesting and hard to explain. Compared with the previous studies[7, 8, 19], the scale of the present study area is much larger. The power-law relationship for the annual data implies that the self-affine property of shoreline changes can exist over four orders of magnitude in alongshore scale, from 10 meters to 3×10^4 meters. As this wide range of scales covers most spatial scales pertaining to the short and medium term coastal evolution, the results suggest that shoreline movements within these scales could be strongly affected by nonlinear shoreline change dynamics including some forms of self-organization.

Since the concept of “self-organization” was introduced by Werner and Fink[1] in their study of beach cusps, models involving self-organization have largely focused on the explanation for the formation of rhythmic features at specific spatial scales, from meters to over 100 km under a prescribed background hydrodynamic conditions[20]. It remains unclear how the self-organization or a combined forced and self-organization mechanism may be used to explain the dynamical changes of shorelines that exhibit power-law scaling[21]. The shoreline change patterns around Hainan Island revealed in this study may provide useful information about spatial and temporal boundaries between self-organization and forcing processes.

Self-organization behavior of coastal morphology

For a complex system involving many processes with different scales which interact on the overlapping spatial scales, the peaks of the shoreline-change power spectra occurring at specific scales may indicate a possible transition of dominant processes but this does not preclude the possibility of a well-organized system with different processes across different scales. For temporal scale one year and spatial scale up to 30 km (May2013-Jun2014), the shoreline change seems to be a result of well-organized system with smooth growth of spectra power along with scales, while the strong seasonal hydrodynamic conditions can cause this trend to break in temporal scale of half year and spatial scale 10-25 km. The evaluation of affecting factors/processes, weak or strong, relies on the temporal and spatial scales considered.

Within alongshore scale 5-30 km, none of azimuth, sediment or deep water wave shows strong correlations with shoreline change (Figure 1 and 6, east and south coast). This indicates that there does no exit a dominant process that is due to any of these factors in the system. The system evolves mainly through internal feedback mechanisms between processes with different spatial scales, *i.e.* through self-organization. And the peaks of spectrum around scale 30 km and beyond are more likely due to other controlling factors of the system.

Controlling role of seasonal hydrodynamic conditions at the scale of 10-25 km

Based on the modelling wave data, tropical cyclones can generate high waves over a large sea surface area: distance between *P1* and *P2* is more than 200 km but high waves driven by cyclones can be easily identified in both positions. The shoreline change in May2013-Dec2013 shows little erosion on east coast, only a part of south coast is seriously eroded. This may be due to the time intervals between the tropical cyclones and the survey, because the cyclones impacted east coast 4 months before the survey in December and their effects have diminished as the result of beach recovery during this period, but the last storm passed south coast in November which is expected to leave a much greater impact on shoreline measured in December.

As it can be expected, high waves induced by cyclones and winter storms can destroy shoreline patterns that had already formed through self-organization process prior to these events after which beach recovery and evolution will resume. This is especially the case for the shoreline changes in May2013-Dec2013 data. As through self-organization process spatial shoreline patterns tend to grow with time, larger scale pattern requires longer time to form than smaller ones[20]. Although there are 1-4 months for shoreline to recovery from impacts of tropical cyclones by Dec 2013, only smaller (less than 10km) shoreline change patterns developed but larger patterns beyond 10km did not have sufficient time to form until Jun 2014.

Geological control at the scales over 30 km

Apart from self-organization and hydrodynamic forcing, the changes in the background coastal settings can also affect the evolution of shoreline, an effect which is often referred to as geological control[22]. Although the correlation is weak between data sets of shoreline change and azimuth, the variation patterns of them do show similar trends on large scales. Beyond the alongshore scale of 30 km, the coastline variation is resulted from the cumulative effects of interactions between hydrodynamic forcing and geological features. As it can be seen shoreline of Hainan Island is divided by various protruding headlands into beach sections of different orientations (Figure 1). While the incoming wave direction from South China Sea is fairly uniform in space, the intersection angle of wave is related to the orientation of local shoreline. Consequently, the sections that have different orientations are affected differently by these hydrodynamic conditions. As a result, the coast sections in four different directions can be clearly identified from the wavelet transform results as shown in Figure 6(c).

Conclusions

Based on the shoreline change data collected at Hainan Island over a 13-month period the analysis reveals that the power-law relationships between the mean variance and the length scale of the annual shoreline changes can hold up to an alongshore scale of 30 km which is several times greater than that has been found in the previous studies[8]. While there is no spatial pattern within the wave direction or significant wave height along the studied coast, the hydrodynamic conditions show significant seasonal character. Five tropical cyclones showed strong impacts on east and south coasts of Hainan Island, and diminished the shoreline change patterns with alongshore scale of 10-25 km. Much of the effects on the shoreline evolution caused by the storm can get averaged out over a time scale of one year, as the long-term shoreline evolution is mostly a diffusive process with diminishing memory effects with time[23]. In the time period of one year, the shoreline change patterns develop into larger spatial scale than seasonal shoreline change patterns, but it is confined by relatively closed bays at scale around 30 km. Furthermore, the coastal orientation changes are also found to be effective in alongshore scale from 40 km to 80 km, or even larger.

It should be pointed out that the shoreline change behavior described has limits as it is based on a coarsely sampled shoreline data from only three surveys over a 13 month period. The results obtained may contain some degrees of uncertainty and are inevitably influenced by the particular morphological characteristics of Hainan Island. More sites with different coastal conditions and data resolutions (spatial and temporal) should be investigated to further establish the scale relationships of shoreline changes on wave-dominated sandy coasts and underlying mechanisms for these changes.

Acknowledgments

This study is carried out as part of a larger project funded by the Public Science and Technology Research Funds Projects of Ocean, China (Grant no. 201405037). The data sets are provided by State Key Laboratory of Estuarine and Coastal Research, ECNU, and requests for materials should be addressed to Shenliang Chen (slchen@sklec.ecnu.edu.cn). The financial support through a joint PhD program awarded to Xiaojing Zhong by the Chinese Scholarship Council and University of Dundee, UK is gratefully acknowledged. The authors would like to thank Jin Hu, Weiheng Zheng, Qing Chen and Wufeng Cheng for their contributions in the field work.

References:

1. Werner, B.T. and Fink, T.M., Beach cusps as self-organized patterns. *Science*, **1993**, *260*, pp.

968-71.

2. Garnier, R., Dodd, N., Falqués, A. and Calvete, D., Mechanisms controlling crescentic bar amplitude. *J. Geophys. Res.*, **2010**, *115*.

3. Tiessen, M.C.H.,Dodd, N. and Garnier, R., Development of crescentic bars for a periodically perturbed initial bathymetry. *J. Geophys. Res.*, **2011**, *116*.

4. Dong, P.,Chen, Y.Q. and Chen, S.L., Sediment size effects on rip channel dynamics. *Coast. Eng.*, **2015**, pp. 124-135.

5. Ashton, A.D. and Murray, A.B., High-angle wave instability and emergent shoreline shapes: 1. Modeling of sand waves, flying spits, and capes. *J. Geophys. Res.*, **2006**, *111*.

6. Lazarus, E.D. and Armstrong, S., Self-organized pattern formation in coastal barrier washover deposits. *Geology*, **2015**, *43*, pp. 363-366.

7. Tebbens, S.F.,Burroughs, S.M. and Nelson, E.E., Wavelet analysis of shoreline change on the Outer Banks of North Carolina: an example of complexity in the marine sciences. *Proceedings of the National Academy of Sciences*, **2002**, *99(suppl 1)*, pp. 2554-2560.

8. Lazarus, E., Ashton, A., Murray, A.B., Tebbens, S. and Burroughs, S., Cumulative versus transient shoreline change: Dependencies on temporal and spatial scale. *J. Geophys. Res.*, **2011**, *116*.

9. Baas, A.C., Chaos, fractals and self-organization in coastal geomorphology: simulating dune landscapes in vegetated environments. *Geomorphology*, **2002**, *48*, pp. 309-328.

10. Southgate, H.N. and Möller, I., Fractal properties of coastal profile evolution at Duck, North Carolina. *Journal of Geophysical Research: Oceans*, **2000**, *105*, pp. 11489-11507.

11. Yang, Z.H., Jia, J.J., Wang, X.K. and Gao, J.H., Characteristics and variations of water and sediment fluxes into the sea of the top three rivers of Hainan in recent 50 years. *Marine Science Bulletin*, **2013**, *32*, pp. 92-99.

12. Wang, B., Chen, S., Gong, W., Lin, W. and Xu, Y., *Formation and evolution of the embayment coasts around Hainan Island*, Ocean Press: Beijing **2006**.

13. Tchernia, P., *Descriptive Regional Oceanography*, Pergamon Press: Oxford, New York **1980**.

14. Zhang, K.,Song, C. and Chen, Y., Records and disaster evaluation of typhoons in east Hainan Island in recent 50 years., **2010**.

15. Boak, E.H. and Turner, I.L., Shoreline definition and detection: A review. *J. Coastal Res.*, **2005**, *214*, pp. 688-703.

16. Friedman, G.M., Dynamic processes and statistical parameters compared for size frequency distribution of beach and river sands. *J. Sediment. Res.*, **1967**, *37*, pp. 327-354.

17. Vincent, L., Dolan, R., Hayden, B. and Resio, D., Systematic variations in barrier-island topography. *The Journal of Geology*, **1976**, *84*, pp. 583-594.

18. Zhou, L.M., Li, Z.B., Lin, M. and Wang, A.F., Numerical simulation of wave field in the South China Sea using WAVEWATCH III. *Chin. J. Oceanol. Limn.*, **2014**, *32*, pp. 656-664.

19. Del Río, L.,Gracia, F.J. and Benavente, J., Shoreline change patterns in sandy coasts. A case study in SW Spain. *Geomorphology*, **2013**, *196*, pp. 252-266.

20. Coco, G. and Murray, A.B., Patterns in the sand: From forcing templates to self-organization. *Geomorphology*, **2007**, *91*, pp. 271-290.

21. Murray, A.B., Lazarus, E., Ashton, A., Baas, A., Coco, G., Coulthard, T., Fonstad, M., Haff, P., McNamara, D., Paola, C., Pelletier, J. and Reinhardt, L., Geomorphology, complexity, and the emerging science of the Earth's surface. *Geomorphology*, **2009**, *103*, pp. 496-505.

22. Jackson, D.W.T.,Cooper, J.A.G. and Del Rio, L., Geological control of beach morphodynamic state.

Mar. Geol., **2005**, *216*, pp. 297-314.

23. Dong, P. and Chen, H., Wave chronology effects on long-term shoreline erosion predictions. *Journal of Waterway, Port, Coast, and Ocean Engineering*, **2001**, *127*, pp. 186-189.

Table 1 *Major capes, rivers along coast of Hainan Island (*based on Yang et al., 2013).*

Type	Water Discharge*	Sediment Discharge*	Name	Flank Profiles
River	5.673×10^9 m^3/y	3.877×10^5 t/y	Nandu	N002, N003
Cape			*Hainanjiao*	N010, N011
Cape			Jingxin (Baohu)	N017, N018
Cape			Tonggu	N024, N025
River	4.780×10^9 m^3/y	4.533×10^5 t/y	Wanquan	N039, N040
Cape			Dahua	N047, N048
Cape			Maliu (Niumiao)	N051, N052
Cape			Lingshui	N061, N062
Cape			Zhuwanxia	N068, N069
Cape			Luhuitou	N069, N070
Cape			Nanshan	N077, N078
Cape			*Yinggeju*	N088, N089
River	3.643×10^9 m^3/y	6.989×10^5 t/y	Changhua	N105, N106
Cape			Lingao	N125, N126

Table 2 *Contributions of the first and second eigenvectors at different coast sections*.

	Profiles	May2013	Dec2013	June2014
Contribution of First Eigenvector (%)	N001~N132	87	88	89
	N010~N049	82	82	86
	N049~N087	89	90	91
	N088~N009	86	89	85
Contribution of First and Second Eigenvectors (%)	N001~N132	95	96	96
	N010~N049	91	93	95
	N049~N087	96	98	97
	N088~N009	95	96	95

Table 3 *Parameters of tropical cyclones passed Hainan Island during investigated period (based on Best Track Data by RSMC Tokyo – Typhoon Center).*

Tropical Cyclone	Maximum sustained wind speed (knot)	Minimum central pressure (hPa)	The longest radius of 30kt winds or greater (nautical mile)	The shortest radius of 30kt winds or greater (nautical mile)
BEBINCA	40	990	150	120
RUMBIA	50	985	180	150
JEBI	50	985	250	150
MANGKHUT	40	992	120	120
HAIYAN	125	895	270	180

Figure 1. Location map of Hainan Island, wave direction contribution around Hainan and routes of tropical cyclones during the investigated period, particle size (D_{50}) of intertidal sediment collected in May 2013 and profile positions. Profiles are numbered N001 to N132 clockwise along the coastline.

Figure 2. Shoreline change around Hainan Island and the results of wavelet analysis. (a) Seasonal shoreline change of May2013-Dec2013 and Dec2013-Jun2014. The ordinate axis indicates shoreline change (negative values - erosion). (b) Wavelet transform results of seasonal shoreline change data with scale parameter a=1. (c) Wavelet transform results of seasonal and annual shoreline change data with scale parameters a=4 and 16. The shaded parts are profiles from N010 to N087 (east and south coasts).

Figure 3. Log-log plots (left) and the corresponding power-spectral exponent β (right) relating wavelet coefficient mean variance of shoreline change to alongshore scale, for profiles N010 to N087. Wavelet width is multiplied by 5 kilometers (distance between every two profiles) to get the alongshore scaling.

Figure 4. EOF analysis of beach profiles around Hainan Island. (a) The weightings of the first and second eigenvectors on each profile in three surveys. (b) First eigenvector of beach profiles. (c) Second eigenvector of beach profiles.

Figure 5. Model results of wave conditions around Hainan. (a) Seasonal significant wave height distribution around Hainan Island, modeled by Zhou *et al.* (2014). (b) and (c) Wave direction and significant wave height at 18.5°N, 110.5 °E (southeast of Hainan) and at 19°N, 108.5 °E (west of Hainan) during survey period, modeled by WaveWatch III (WW3) Global Wave Model.

Figure 6. Wavelet analysis of annual shoreline change, azimuth and submerged slope of alongshore profiles. Wavelet coefficients of azimuth are divided by three for plotting in figures. Submerged slope is calculated between elevations 0 and -5 m at each profile.

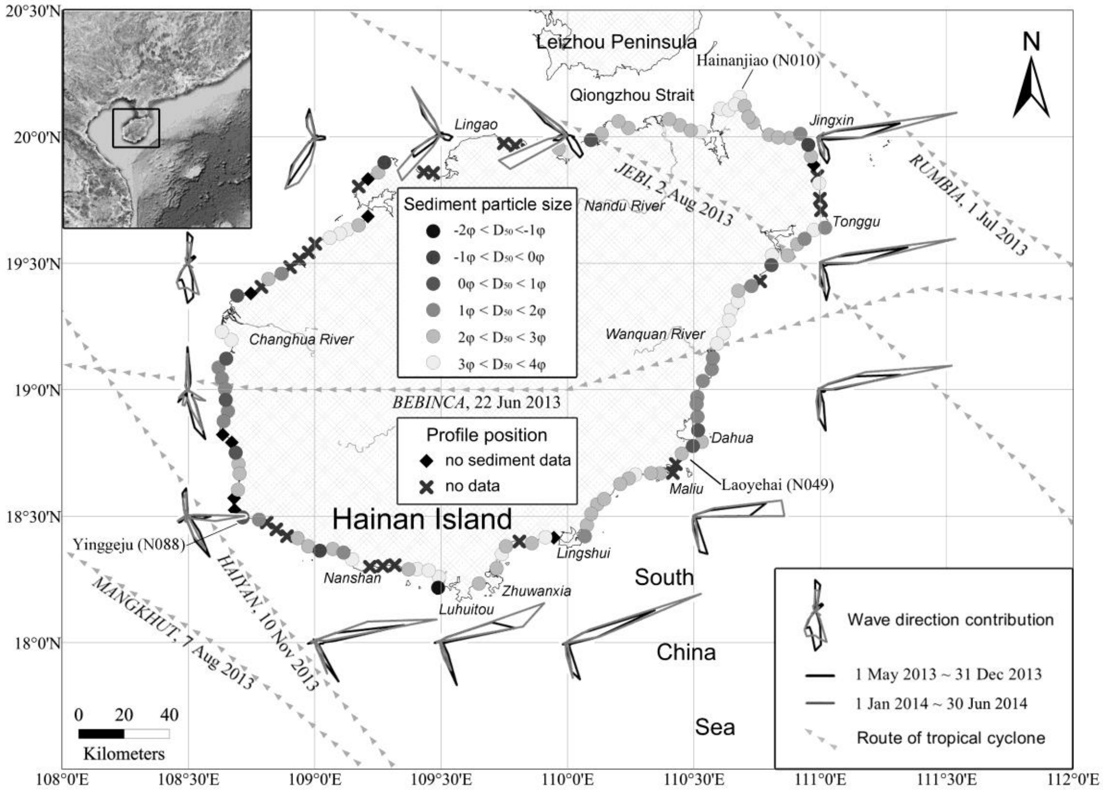
20°30'N
20°0'N
19°30'N
19°0'N
18°30'N
18°0'N
108°0'E
108°30'E
109°0'E
109°30'E
110°0'E
110°30'E
111°0'E
111°30'E
112°0'E
N
Leizhou Peninsula
Hainanjiao (N010)
Qiongzhou Strait
Lingao
Jingxin
Nandu River
JEBI, 2 Aug 2013
RUMBIA, 1 Jul 2013
Tonggu
Changhua River
Wanquan River
BEBINCA, 22 Jun 2013
Dahua
Laoyehai (N049)
Maliu
Hainan Island
Yinggeju (N088)
Lingshui
Nanshan
Zhuwanxia
Luhuitou
HAIYAN, 10 Nov 2013
MANGKHUT, 7 Aug 2013
South
China
Sea
0 20 40
Kilometers
Sediment particle size
-2φ < D50 <-1φ
-1φ < D50 < 0φ
0φ < D50 < 1φ
1φ < D50 < 2φ
2φ < D50 < 3φ
3φ < D50 < 4φ
Profile position
no sediment data
no data
Wave direction contribution
1 May 2013 ~ 31 Dec 2013
1 Jan 2014 ~ 30 Jun 2014
Route of tropical cyclone

Figure 1

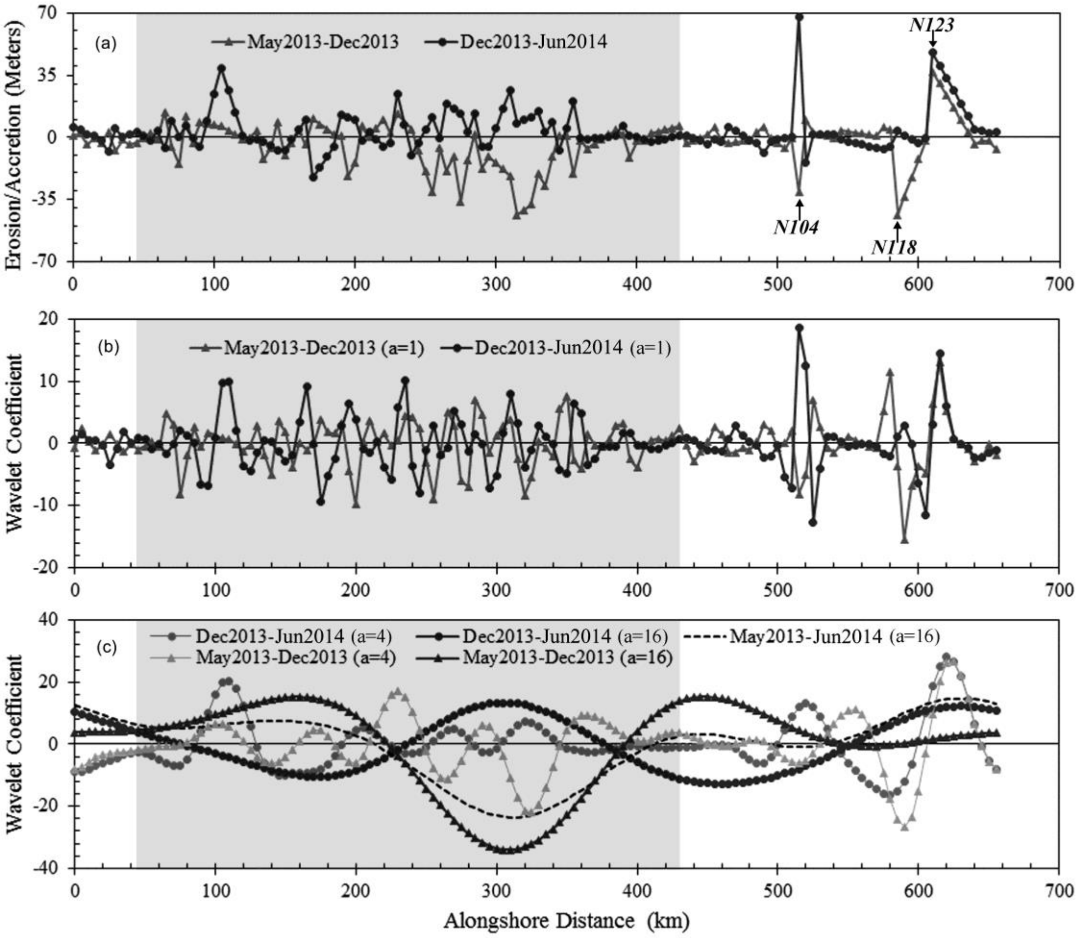
(a)
May2013-Dec2013
Dec2013-Jun2014
N123
N104
N118
Erosion/Accretion (Meters)
70
35
0
-35
-70
(b)
May2013-Dec2013 (a=1)
Dec2013-Jun2014 (a=1)
Wavelet Coefficient
20
10
0
-10
-20
(c)
Dec2013-Jun2014 (a=4)
Dec2013-Jun2014 (a=16)
May2013-Jun2014 (a=16)
May2013-Dec2013 (a=4)
May2013-Dec2013 (a=16)
Wavelet Coefficient
40
20
0
-20
-40
0
100
200
300
400
500
600
700
Alongshore Distance (km)

Figure 2

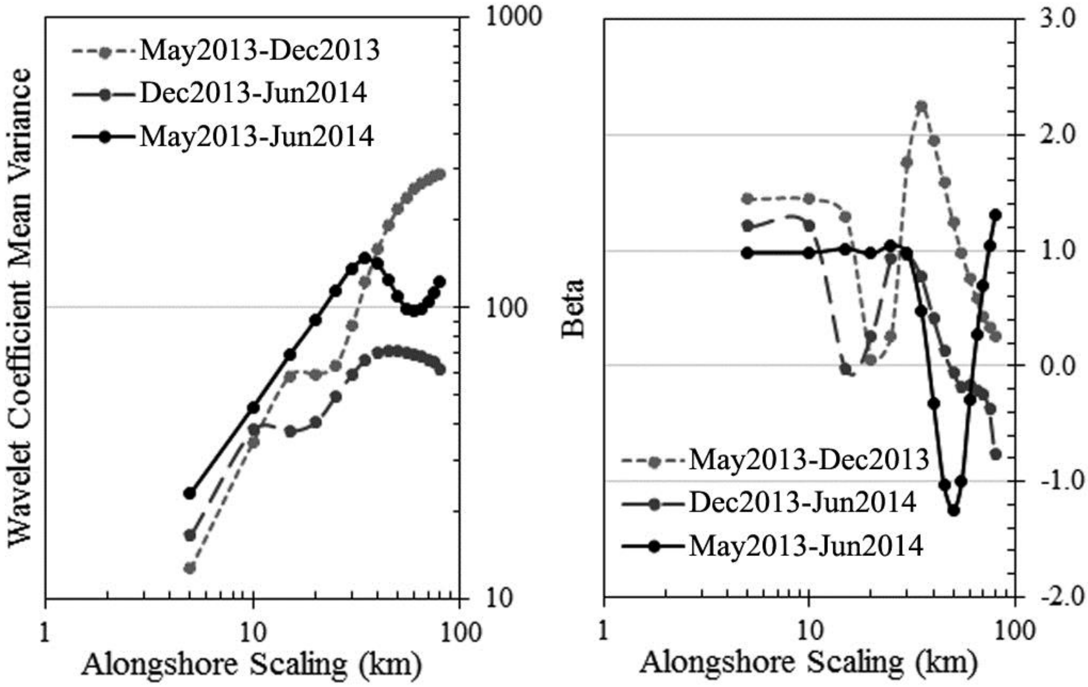
May2013-Dec2013
Dec2013-Jun2014
May2013-Jun2014
Wavelet Coefficient Mean Variance
1000
100
10
1
10
100
Alongshore Scaling (km)
Beta
3.0
2.0
1.0
0.0
-1.0
-2.0
1
10
100
Alongshore Scaling (km)
May2013-Dec2013
Dec2013-Jun2014
May2013-Jun2014

Figure 3

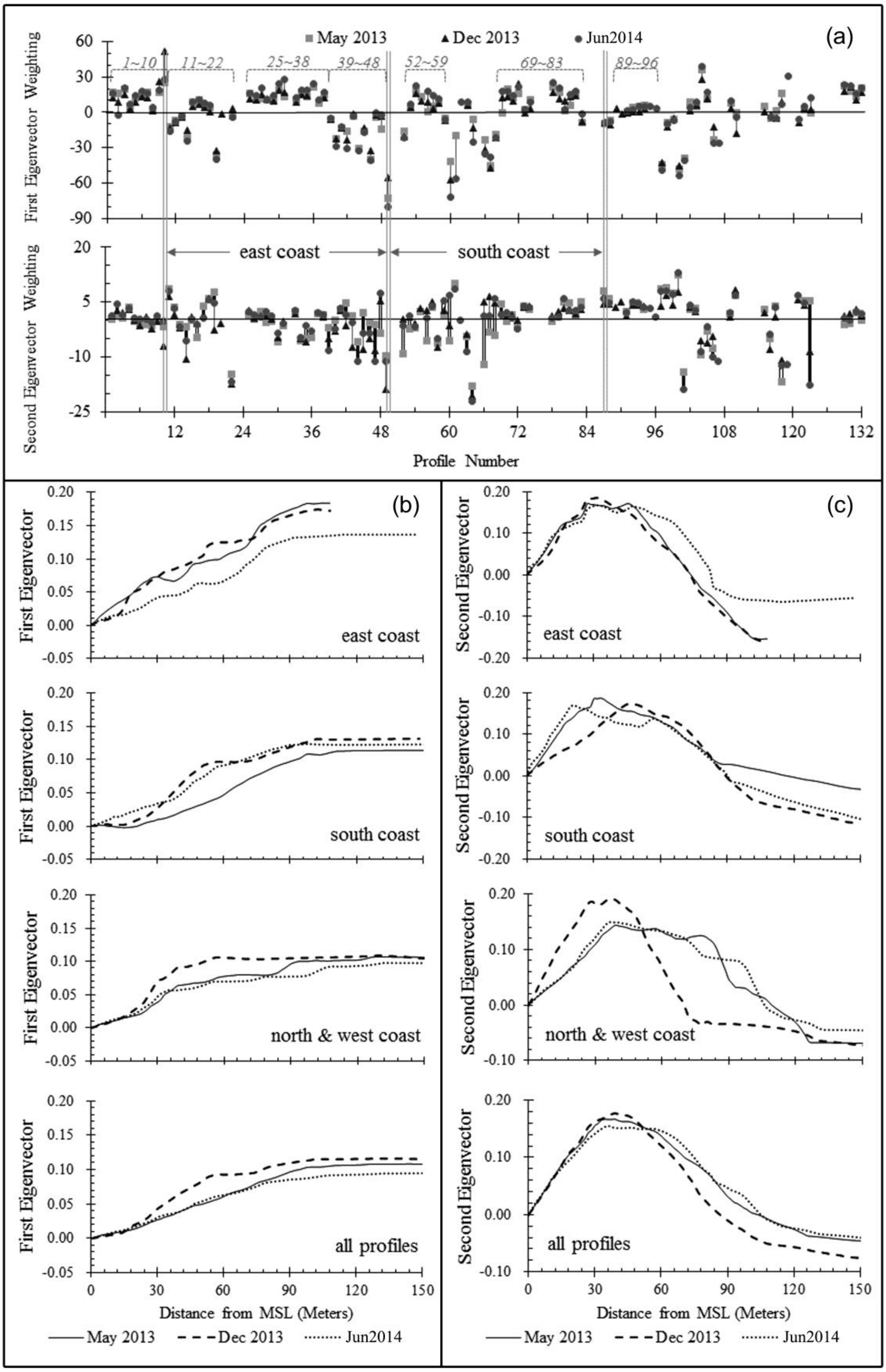
(a)
May 2013
Dec 2013
Jun2014
1~10
11~22
25~38
39~48
52~59
69~83
89~96
First Eigenvector Weighting
60
30
0
-30
-60
-90
Second Eigenvector Weighting
20
5
-10
-25
east coast
south coast
12
24
36
48
60
72
84
96
108
120
132
Profile Number
(b)
(c)
First Eigenvector
Second Eigenvector
east coast
south coast
north & west coast
all profiles
0.20
0.15
0.10
0.05
0.00
-0.05
-0.10
-0.20
0
30
60
90
120
150
Distance from MSL (Meters)
May 2013
Dec 2013
Jun2014

Figure 4

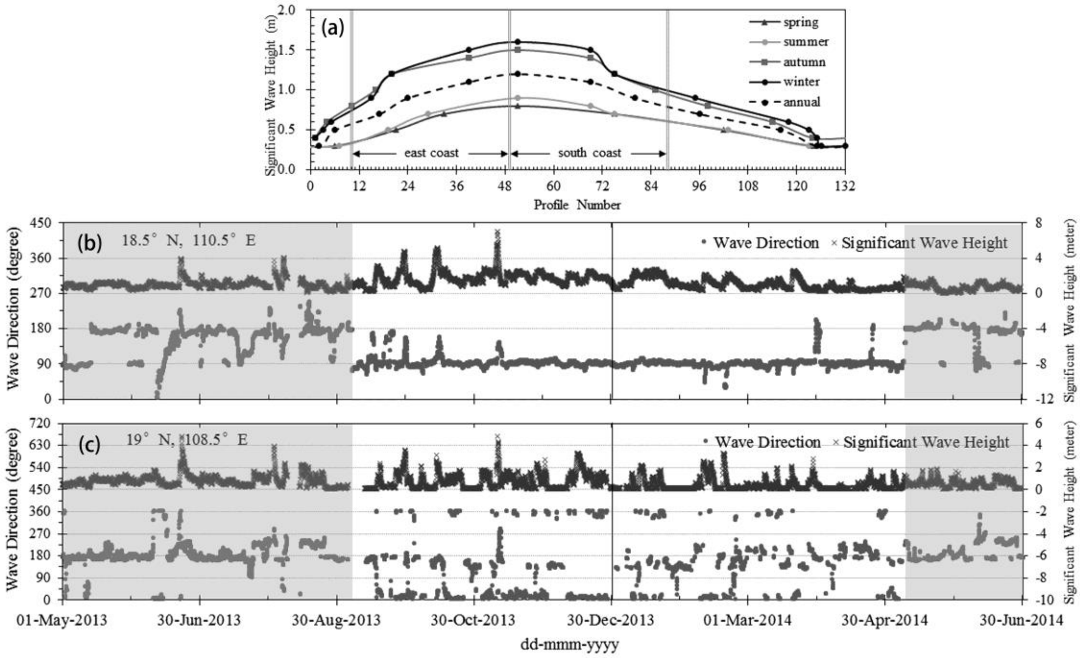
(a)
Significant Wave Height (m)
spring
summer
autumn
winter
annual
east coast
south coast
Profile Number
(b)
18.5° N, 110.5° E
Wave Direction
Significant Wave Height
Wave Direction (degree)
Significant Wave Height (meter)
(c)
19° N, 108.5° E
dd-mmm-yyyy
01-May-2013
30-Jun-2013
30-Aug-2013
30-Oct-2013
30-Dec-2013
01-Mar-2014
30-Apr-2014
30-Jun-2014

Figure 5

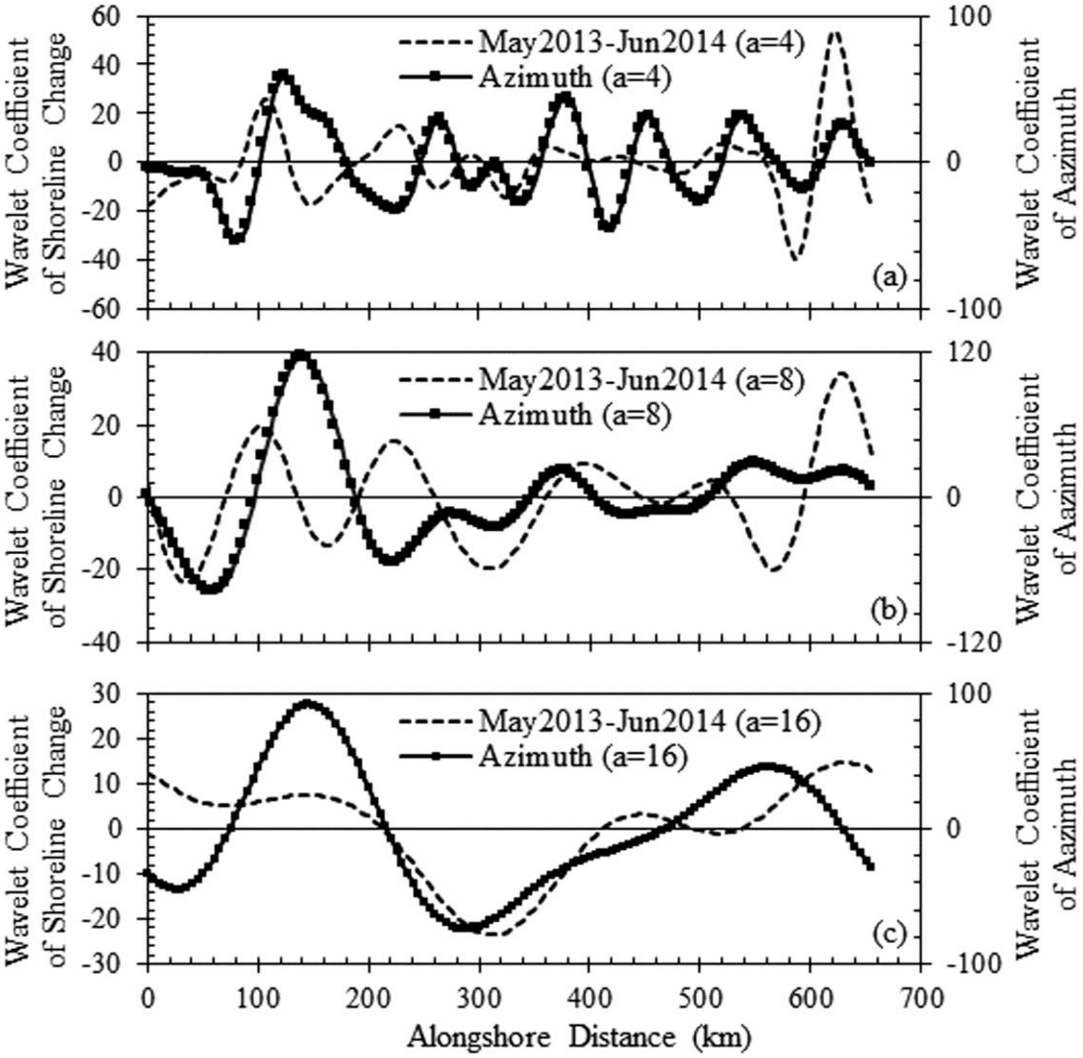
Wavelet Coefficient of Shoreline Change
Wavelet Coefficient of Aazimuth
May2013-Jun2014 (a=4)
Azimuth (a=4)
(a)
60
40
20
0
-20
-40
-60
100
0
-100
May2013-Jun2014 (a=8)
Azimuth (a=8)
(b)
40
20
0
-20
-40
120
0
-120
May2013-Jun2014 (a=16)
Azimuth (a=16)
(c)
30
20
10
0
-10
-20
-30
100
0
-100
0
100
200
300
400
500
600
700
Alongshore Distance (km)

Figure 6